SLAC-PUB-623
July 1969
(EXPI)

MECHANISM OF SECONDARY EMISSION AND SINGLE PARTICLE STATISTICS FROM LOW DENSITY FILMS OF ALKALI HALIDES*

E. L. Garwin and J. Llacer
Stanford Linear Accelerator Center
Stanford University, Stanford, California 94305

(Submitted to J. Appl. Phys.)

*Work supported by the U. S. Atomic Energy Commission.

ABSTRACT

The mechanism of field enhanced secondary emission has been studied experimentally in detail for KCl low density transmission dynodes transferred in a dry nitrogen atmosphere. By means of a Kelvin probe located at the center of a collector, dynode surface potentials and their relationship with collector potential, secondary yield, primary energy and current density have been studied. A unique relationship between yield and surface potential has been found, independent of all other parameters for current densities between 1 and 10 nA/cm^2. This study clearly shows that an avalanche process, together with an increase in escape length, is responsible for the high yields obtainable. A study of transient effects reveals that the high surface potential needed for high yield decays rapidly after the primary beam is turned off. A smaller surface potential, with a long decay time constant, can be expected to provide slight field enhancement for single particle bombardment at low rates. The statistical distributions of the number of emitted secondary electrons per primary incident at high (1-MeV) and low (9.5-keV) energies have been measured for low density films of CsI and KCl at low count rates. The results do not differ very much from those obtained previously from normal density films except that the yields are somewhat higher, particularly after the film has been charged with a dense primary beam. The distributions obtained are non-Poissonian in nature (more nearly exponential), and this is explained by their similarity to normal density films.

I. INTRODUCTION

In the last few years there has been substantial activity in the study and application of low density (smoke) films of some insulators as high yield secondary emitters. These films exhibit secondary emission coefficients which are dependent not only on the energy of the primary electrons, but also on the current density, time, and the potential of the collector. The most complete study to date has been carried out by Green, Boerio, and Goetze[1,2] on KCl in transmission dynodes. Fabrication techniques, measurements of the dependence of yield on the various parameters, some phenomenological theories explaining the observed facts, and a discussion of applications have been given by those authors. However, a controversy remained regarding the basic nature of field enhanced secondary emission from KCl, and presumably from other alkali halides. When the potential of the exit surface of a transmission dynode becomes positive under bombardment with primary electrons (collector positive with respect to dynode substrate), does the enhancement of the yield result only from an increase of the depth from which internal secondaries can escape, or is there an avalanche mechanism under the action of the internal electric field. This question becomes important in considering applications in which the statistical distribution of emitted secondaries is relevant, as in the problem of identifying relativistic particles with equal momentum but different energies,[3] or in predicting noise figures for low-density multiplier structures.

It is the purpose of this paper to present the results of experiments which resolve the above controversy, and allow evaluation of low density transmission dynodes as emitters for low or high energy single particle counting. The experiments are: (1) a careful measurement of the relationships between yield, surface potential, collector potential, and dynode-to-collector spacing by means of a tube containing a Kelvin probe in the collector, and (2) measurement of the statistical number distribution of secondaries from 1-MeV and 9.5 keV single primary electrons under conditions of varying collector potential and correspondingly changing yield. The requirements in terms of current density for obtaining high yields are also investigated.

Practical transmission dynodes consisting of a 1000 Å Al_2O_3 support film, 500 Å of Al for the back contact, and low density deposits of KCl have been investigated. Statistics measurements on CsI have also been made. After fabrication by standard techniques,[2] in oil free vacuum systems, films have been transported to the measuring apparatus in a dry N_2 atmosphere (less than 1.5% relative humidity). After pump down first with chilled molecular sieve, and finally with ion pumps to about 10^{-8} torr, measurements are initiated. The results presented are for unbaked films since tests carried out after baking the systems to 150°C for over 48 hours showed no significant difference in the results.

II. MEASUREMENT OF SURFACE POTENTIAL

The mechanism of charge build-up and storage in practical low density films of KCl has been studied by means of a Kelvin probe. When a small vibrating probe is placed at the center of a planar collector located near the exit surface of a transmission dynode, a small ac signal proportional to the average potential difference between the collector and the surface of the dynode will be developed. By proper choice of the phase between the signal driving the probe and the reference signal at the lock-in detector it is possible to render the probe insensitive to the presence of electrons in the space between the dynode and the collector. A tube for the measurement of the relationships between secondary yield, collector potential and the state of charge of the dynode has been developed, and has been described in detail in Refs. 4 and 5. The measurement capabilities of the tube as used in the present experiments can be summarized by indicating that it is possible to measure a surface potential difference V_S between exit and substrate sides of a transmission dynode of up to 100 volts with an accuracy of ± .5 volts. Risetimes in the potential of the order of milliseconds are observable by the use of a storage oscilloscope for recording the output. Collector-to-dynode spacings between .2 and 2 mm and primary electron energies between 5 and 12 keV at currents between 1 and 100 nA, with uniform illumination over a cross section of 1 cm^2 can be used. The measurements of secondary emission yield are estimated to be accurate within ± 10%.

For the steady state results, the collector to dynode substrate potential, V_C, has been swept from 0 to + 100 volts at a very low rate (several minutes) to insure that charging effects with very long time constants are accurately recorded. For transient studies, the primary beam was turned on and off by means of a mercury relay switch acting on the control electrode of the simple Pierce-type electron gun. Beam current risetimes of 2.5 milliseconds were then obtained.

A. Steady State Results

Figure 1 shows a set of curves of transmission yield δ_t vs collector potential as a function of primary energy E_p for a typical KCl film with density approximately 3% of bulk density and thickness 120 $\mu g/cm^2$. Transmission yield is defined as the secondary yield δ plus the transmission coefficient η_t. For high gain dynodes $\delta_t \simeq \delta$. I_p is the primary current. The set of curves, showing pronounced changes in slope, is characteristic of a large number of KCl low density dynodes made at the Stanford Linear Accelerator Center. For the same set of measurements, the relationship between the potential at the exit surface of the dynode V_S (with dynode substrate at zero potential) and collector potential V_C is shown in Fig. 2. It is apparent that there exists a maximum amount of positive charge stored in the dynode which depends on primary energy. Saturation of this maximum occurs when the primary electrons are almost fully penetrating, at $E_p = 8$ keV. The same set of curves, including the saturation of V_S is obtained when I_p is increased by one order of magnitude.

Figure 3 combines the results of Figs. 1 and 2 to show the relationship between δ_t and V_S for points taken from the curves of $5 < E_p < 8$ keV, and for points from similar measurements at different spacings, d. The unique relation between yield and surface potential becomes quite apparent in Fig. 3, which shows complete independence on spacing and on primary energy in the region measured. The only exception occurs when saturation of V_S occurs at a particular E_p. Then, a sharp increase in yield takes place without further increase in V_S. This has the character of a breakdown, although it is not destructive. The appearance of two regions I and II, of distinctly different slope in Fig. 3 indicates that a threshold mechanism is active in generating the high values of δ_t observed in these films. It must be pointed out, however, that the pronounced changes in slope become much less abrupt, and therefore less observable, as the film ages.

The state of charge can be reduced to zero volts at any time by running the primary beam with the zero collector-to-dynode potential for a few seconds.

B. Transient Response

As pointed out by Goetze, Boerio, and Green[2] there are two main response times in KCl low density dynodes: a fast part (risetime less than 1 nanosecond[6] when the film is maintained fully charged) and a slow part, with risetimes of the order of seconds when V_C is changed. Our results show that these two forms of behavior are intimately related to the two main regions of different slope in the graph of δ_t vs V_S of Fig. 3. As long as the conditions of the experiment (E_p, V_C, d) were such that transmission yield would be below approximately 15, and V_S below approximately 35 volts under steady state conditions (Region I in Fig. 3) the final value of V_S obtained under bombardment would remain fixed with the primary beam turned off for periods of at least 24 hours. Moverover, when the beam was again turned on, full gain would be obtained within the 2.5 milliseconds primary beam risetime. This is shown in Fig. 4, for E_p = 6 keV, d = .5 mm, V_C = 100 volts. When the beam is turned on with the dynode in an uncharged condition, the yield has become approximately 9 and the film has charged to nearly 20 volts after 50 seconds as shown in Fig. 4a. After the beam is turned off the charge state remains as shown in Fig. 4b. Finally in Fig. 4c, the beam turn-on from the charged condition is observed with practically full gain. In contrast, when operating conditions place the system in Region II (higher slope) of Fig. 3, the final value of V_S before beam turn-off is not sustained, but decays to a value somewhat dependent on the individual parameters. This is shown in Fig. 5 for E_p = 8 keV, d = .5 mm, V_C = 60 volts. After beam turn-on from an uncharged condition (Fig. 5a), a yield of 20 and a charging potential of approximately 42 volts are observed. After beam turn-off (Fig. 5b), V_S decays to about 18 volts. From that condition, Fig. 5c shows the reestablishing of final conditions of Fig. 5a within .5 seconds of beam turn-on, the yield exhibiting a peculiar transient which has been observed repeatedly in the high yield region of operation. On this same time scale (.1 sec/cm.) the effect of turning the beam off and on again within .5 seconds is shown in Fig. 5d, where both yield and V_S behave as if the beam had not been cut off at all. On a faster time scale (1 millisecond/cm), turning the beam on after several minutes, Fig. 5e, or after .5 seconds, Fig. 5f, from turn-off shows that the respective initial yields are nearly identical. The difference, however, becomes more substantial at operation with higher steady state yields. Small instrumental drifts and differences in oscilloscope triggering times are observable in Figs. 4 and 5. A small deterioration of the film characteristics is observable by comparing the yields of Figs. 4 and 5 with those of Fig. 1.

The dependence of the observed phenomena on spacing, d, and primary current, I_p can be summarized as follows: All other conditions remaining equal, increased spacing results in lower final yields and longer duration of transients, showing the important role of the electric field between dynode and collector. An order of magnitude increase in primary current mainly speeds up the transient effects, both in the yield and surface charge.

III. MEASUREMENT OF SINGLE PARTICLE STATISTICS

The object of this experiment has been the measurement of the probability P(n) that n electrons are emitted from a practical low density transmission dynode when one primary electron strikes it. The measurement of this probability distribution for normal desnity films of CsI, KCl, and LiF has recently been published by Llacer and Garwin.[7] The same techniques have been used for the present low density case. The secondary electrons resulting from a single primary are accelerated through a 23.5 keV potential and strike the entrance face of a surface barrier lithium-drifted-silicon radiation detector. The energy deposited in the detector is proportional to the number of secondaries generated at the test dynode. This information is stored in a multichannel analyzer. Measurements have been carried out on a variety of low density films of CsI and KCl. Primary electrons of approximately 1-MeV of energy from a $Sr\text{-}Y^{90}$ source (selected by the energy deposited in a second semiconductor detector) have been used in a coincidence method so that it has been possible to measure P(0) accurately for that primary energy. For measurements near the peak of secondary yield, single 9.5-keV electrons from a low temperature filament have been used. More complete details on the methods used and on the estimates of errors appear in Ref. 7.

Because of the expected charging of the films under bombardment the following sequence of measurements has been adhered to for each particular film:

(a) Measurements at low counting rate starting from a fresh uncharged film, with both high and low energy primaries. (A few thousand counts per second.)

(b) Measurement of secondary yield at 9.5-keV primary energy with current densities of 1-10 nA/cm^2.

(c) With the film left in a charged condition from the previous measurement, (long decay time part) measurements are made again at low counting rates.

The above series of measurements has been carried out at each of several voltages applied to a grid placed at the exit side of the dynode to study the effect of the "collector" potential on the statistical distributions. Measurements (b) were made in order to verify that the films being measured exhibited the normal field-enhanced yield behavior and for the purpose of leaving them charged, and those results need not be reported.

The results of P(n) at low counting rates for low density films of both CsI and KCl have been characterized by small changes in the distributions as a function of grid voltage V_G. Systematic measurements at low counting rates taken a short time after the films were charged with a dense low energy beam have only been obtained with CsI films. With KCl dynodes, a very substantial Malter emission[8] ($\sim 10^5$ counts per second) appeared after the charging beam was turned off and only after 30 to 60 minutes was it possible to measure statistical distributions without significant interference from chance coincidences. Figure 6a shows results from an initially uncharged film of CsI for 1-MeV primaries, while Fig. 6b shows the distributions obtained at times, t, of 7 minutes and 67 minutes after the charging beam was cut off. Figure 7 shows results obtained from CsI with 9.5-keV primary electrons, first from an uncharged film, and then at various times after charging. Measurements of P(n) for KCl films are shown in Figs. 8 and 9 which are for uncharged films at high and low primary energies respectively, and in Fig. 10 which shows the long term effects of charging on the distributions. Our experiments show that increasing both the density and thickness of the films produces very little difference in the observed probability distributions, although such films usually have slightly higher yields. Since P(0) cannot be measured directly at low energies, all the graphs for E_p = 9.5-keV have been normalized to unit area between n = 1 and 35. The values of P(n) and δ presented in Figs. 7 and 9, are therefore optimistic; true values are obtained by dividing by (1 + P(0)). Since P(0) is lower at 1 MeV in low density than in normal density films[6] one could expect that a similar relationship would hold at low primary energies. If this is so, P(0) for low density films should be less than .3 in CsI and less than .65 in KCl, those figures being the ones obtained for normal density dynodes.[7]

IV. EFFECT OF CURRENT DENSITY ON YIELD

After observing that the yield at low counting rates does not exhibit the very large enhancement observable with dc beams at current densities of the order of nanoamps per cm^2, measurements with increasing current density at 9.5-keV primary energy were carried out, and the ratio of the yields at two different grid voltages (V_G) were recorded. A sample of the results for KCl is given in Fig. 11. It is clear that full enhancement is only obtained at current densities above 1 nA/cm^2. The results for CsI show that maximum gain is only obtainable at even higher densities, near 10 nA/cm^2. At a primary current density of .4 nA/cm^2 the ratio $\delta(V_G = 90 \text{ volts}) / \delta(V_G = 9 \text{ volts})$ is 1.4, which is very nearly the same as found at the low counting rates of the experiments in Section III. These results explain the low yields obtained at low counting rates for both high and low energy primaries. In contrast, the gain of KCl low density films for minimum ionizing particles at current densities of approximately 4×10^{-8} A/cm^2 was found to be from 5 to 6 by Garwin and Edgecumbe,[3] and at low primary energies (8 keV), Dietz, Hanrahan, and Hance[9] obtained yields of approximately 30 at current densities of 10^{-6} A/cm^2.

V. DISCUSSION OF RESULTS

A quantitative description of the mechanism involved in field enhanced secondary emission from low density films is quite complicated and will not be attempted here. The energy loss suffered by primary electrons and the electron-phonon interaction which determine both the escape probability of internal secondary electrons and their statistical distribution have been studied in detail in Refs. 4, 5, and 7 for normal density films of alkali halides. Those results are used below to obtain a qualitative description of the principal phenomena taking place in low density films.

In the absence of substantial field enhancement, low density films behave in a way very similar to normal density films, with the added feature that the long filaments of microcrystallites increase the effective area from which electrons can escape, and thereby the yield is increased. For example, the statistical distributions of the number of secondaries emitted per primary from normal density films of CsI[7] are very similar to the ones shown here in Figs. 6a and 7 for initially uncharged low density films of the same material. At $E_p = 1$ MeV the yield for a normal density film of 500 Å was measured to be .68, while the low density film of Fig. 6a gives $\delta = .99$ at $V_G = 9$ volts. P(0) has been reduced in the low density case to about 0.70 from 0.80 which accounts for the yield increase.

When the primary current, collector voltage and spacing are set for operation in Region I of Fig. 3, charge and secondary yield are determined by mechanisms involving hole trapping, drift of electrons under the action of the electric field (in addition to their diffusion motion), recombination of electron-hole pairs, and conditions set at the alkali halide-metallic substrate interface. It is proposed that in Region I, the main effect of these mechanisms is an enhancement by the internal electric field of the depth from which electrons escape.

The behavior of films in Region II of Fig. 3 is characterized by the fact that the slope of δ_E vs V_S is twice that of Region I and that the change in slope occurs at a well defined point. This is consistent with the continuing yield enhancement mechanism of Region I operating on the internal secondaries as V_S increases in Region II, but with an increasing fraction of those secondaries undergoing multiplication by a factor of two. At the end of Region II ($V_S \approx 70$ V), the extrapolated yield without multiplication would be $\delta_E \approx 30$. Apparently one-half of these electrons actually multiply, going a measured yield near 45 as shown in Fig. 3. The process of multiplication (avalanching) should have a threshold at $V_S = (E_g + \chi)$, where E_g is the band gap and χ the electron affinity. For KCl this threshold should be approximately 8.5 eV as has been observed in measurements of δ_t vs V_C carried out in a diffusion-pump vacuum system a few minutes after "in situ" evaporation.[10] Figure 12 shows these results for a film comparable to the ones measured in this work. V_E is the exit surface potential estimated from considerations developed by Goetze et al.,[2] The substantial difference in the details of the yield curves of a fresh film and one transferred in a dry nitrogen atmosphere can only be the object of some speculation: The film thickness (120 $\mu g/cm^2$) is much larger than the escape depth of electrons measured in a field-free case (5 to 10 $\mu g/cm^2$, Ref. 5). The results are explained if in transferred films, internal secondaries do not have the full surface potential available for acceleration and avalanching. In a fresh film, however, there must exist a large field-free region deep in the film, with a dipole layer which is of a thickness comparable to the escape depth, and which is located at the exit surface.

As V_C is increased to the point of maximum surface potential, high electric fields lead to increased yield which, in turn, leads to higher fields created by trapped holes which do not have the opportunity to recombine as the electrons are swept away by the internal field. The limiting mechanism must be determined by non-linear conductivity of the film at high fields, i.e., a process which brings sufficient electrons to the neighborhood of the holes for them to recombine and prevent further charging. Malter emission from the substrate could provide such currents. In fact, as indicated above, substantial Malter emission has been observed in freshly charged KCl low density films. Another non-linearity which is not explainable at present is the observed dependence of field enhanced emission with current density. Its effects, as well as the fact that CsI and KCl low density films do not retain their high state of charge are very strong determining factors on the measured statistical distributions of emitted secondaries. As discussed in detail in Ref. 7, the statistical distributions from normal density films of alkali halides are not Poissonian in character. A Poisson-like distribution would be very desirable from the point of view of applications involving single particle counting. It is clear from the present results that low counting rate field enhancement effects in low density dynodes do not alter the emission statistics substantially. Low density films are therefore not particularly better suited for single particle counting than normal density films. At high counting rates, Dietz, Hanrahan, and Hance[9] have already shown that the distributions are still nearly exponential in nature.

VI. CONCLUSION

In this paper experiments have been reported whose results help in the understanding of the complex phenomenon of field-enhanced secondary emission from low density transmission dynodes. In particular, a study of the relationship between secondary yield and potential at the exit surface of the dynodes indicates that the high yields of these dynodes can be attributed both to an enhancement in the probability of escape of internal secondary electrons and to an avalanche process which multiplies the number of internal secondaries. It has also been shown that the high yields are not attainable at low count rates, so that the statistical distributions of secondaries emitted in response to single particles of low or high energy (9.5-keV and 1-MeV) are not very different from the distributions obtained from films of normal density.

ACKNOWLEDGEMENTS

The authors would like to thank A. Roder and Charles L. Thurman, at the Stanford Linear Accelerator Center, for their assistance in making the complete dynodes, and carrying out some of the measurements reported.

REFERENCES

1. M. Green, A.H. Boerio, and G.W. Goetze, "Research on high gain transmission secondary emission films," Westinghouse Research Report No. 64-9Z27-252-R1, USAERDL, Fort Belvoir, Virginia.
2. G.W. Goetze, A.H. Boerio, and M. Green, J. Appl. Phys. 35, 482 (1964).
3. E.L. Garwin and J. Edgecumbe, Advances in Electronics and Electron Physics 22 (1966).
4. J. Llacer, "Transmission secondary emission from thin films of alkali-halides," Report No. SLAC-86, Stanford Linear Accelerator Center, Stanford University, Stanford, California (1968).
5. J. Llacer and E.L. Garwin, (to be published in J. Appl. Phys. June 1969).
6. E.J. Sternglass and G.W. Goetze, IRE Trans. Nucl. Sci. 9, 97 (1962).
7. J. Llacer and E.L. Garwin, (to be published in J. Appl. Phys. Sept. 1969).
8. L. Malter, Phys. Rev. 50, 48 (1936).
9. L.A. Dietz, L.R. Hanrahan, and A.B. Hance, Rev. Sci. Inst. 38, 176 (1967).
10. E.L. Garwin and J. Edgecumbe, Bull. Am. Phys. Soc. 10, 725 (1965).

LIST OF FIGURES

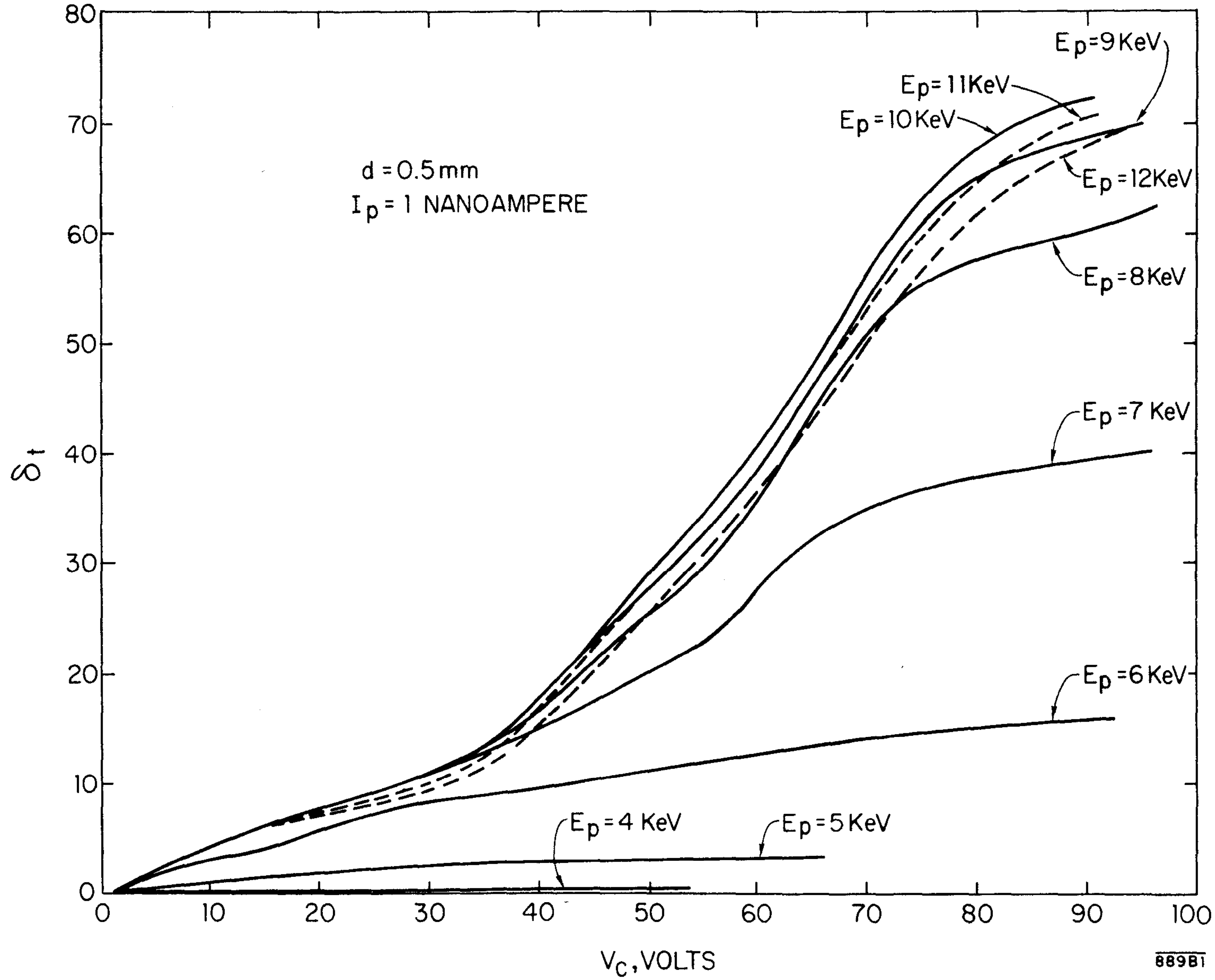

80
70
60
50
40
30
20
10
0
δ_t
0
10
20
30
40
50
60
70
80
90
100
V_C, VOLTS
d = 0.5 mm
I_p = 1 NANOAMPERE
E_p = 9 KeV
E_p = 11 KeV
E_p = 10 KeV
E_p = 12 KeV
E_p = 8 KeV
E_p = 7 KeV
E_p = 6 KeV
E_p = 4 KeV
E_p = 5 KeV
889B1

Fig. 1

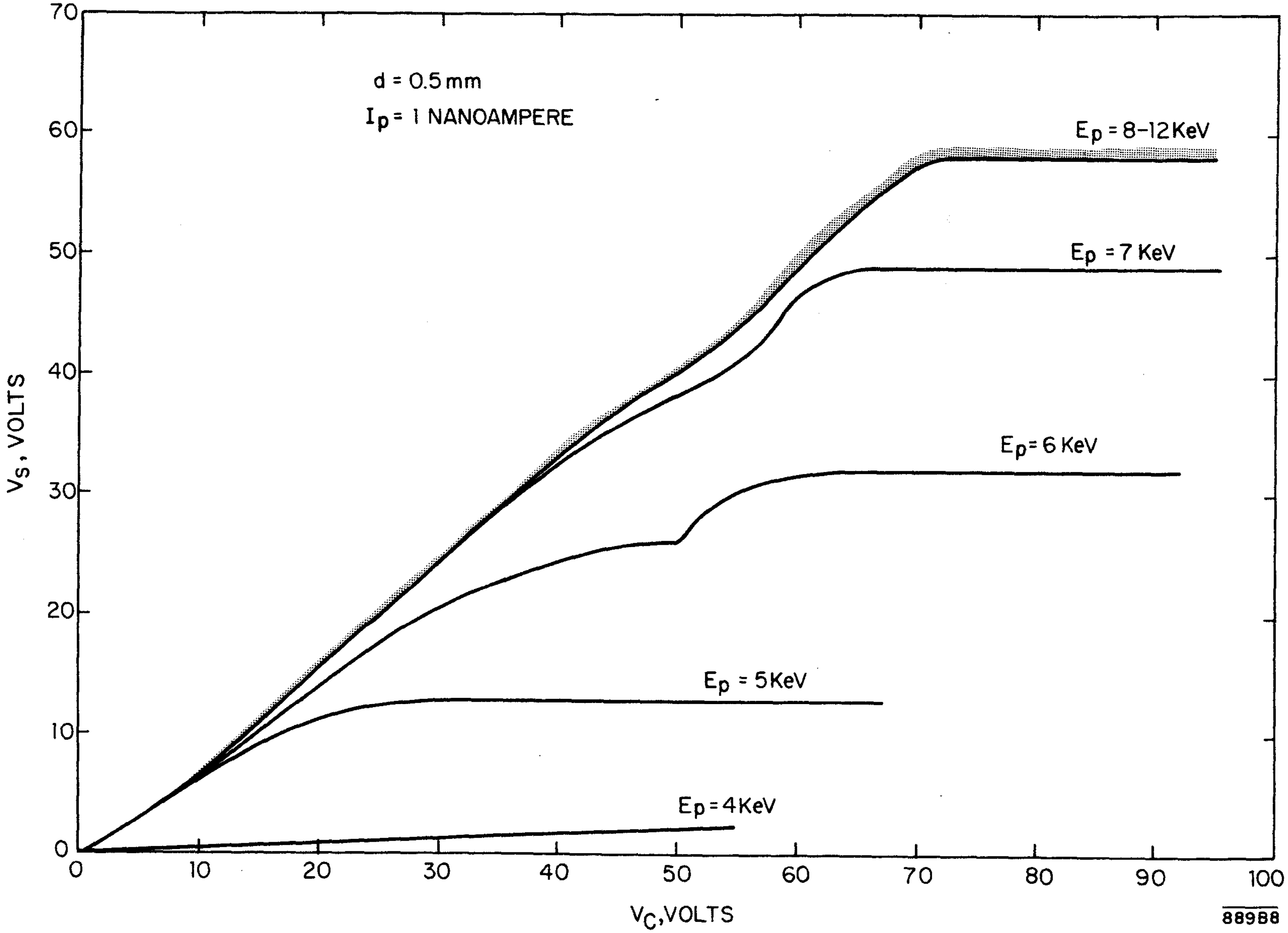

d = 0.5 mm
Ip = 1 NANOAMPERE
Ep = 8-12 KeV
Ep = 7 KeV
Ep = 6 KeV
Ep = 5 KeV
Ep = 4 KeV
Vs, VOLTS
VC, VOLTS
0
10
20
30
40
50
60
70
80
90
100
889B8

Fig. 2

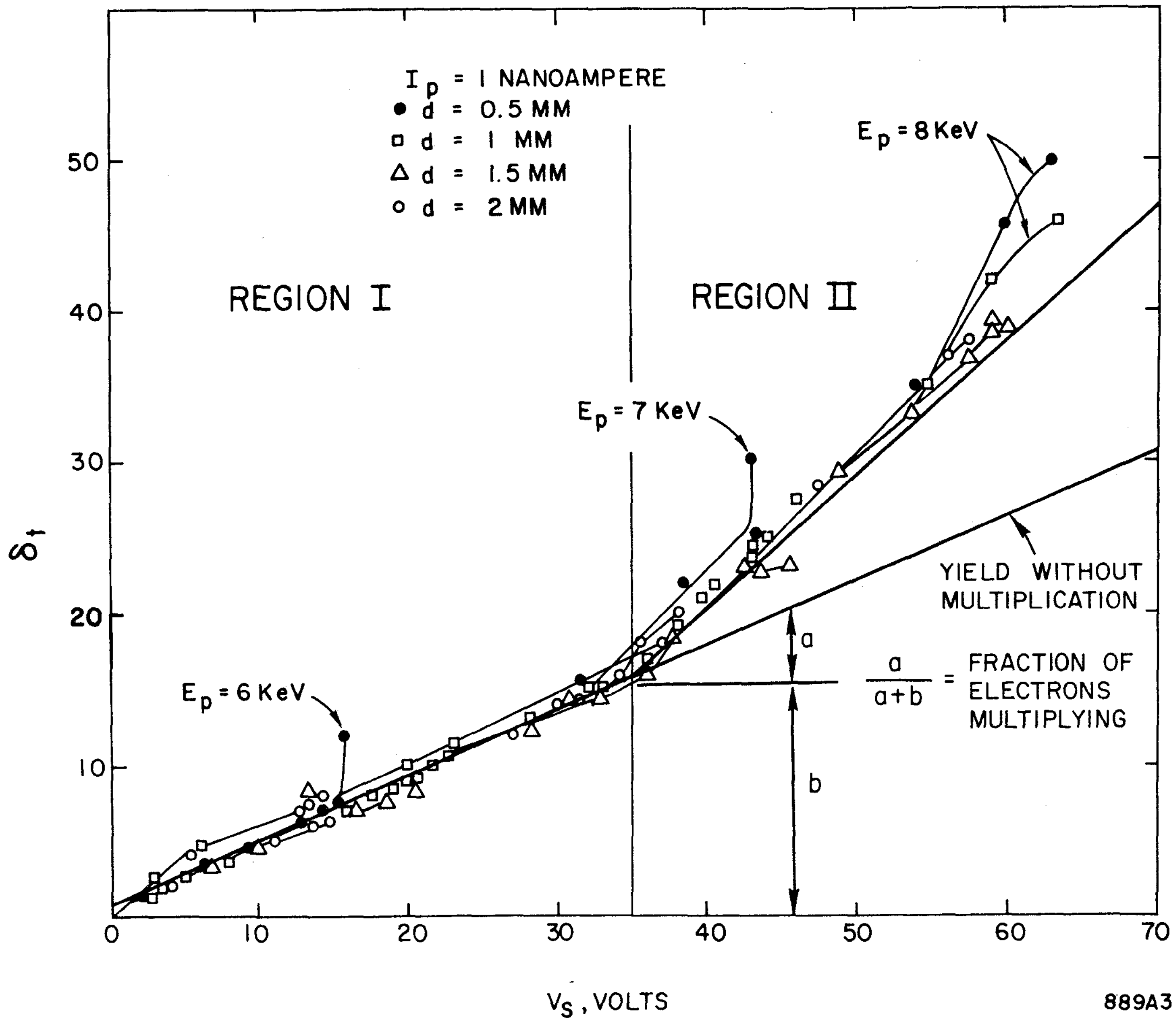

I_p = 1 NANOAMPERE
● d = 0.5 MM
□ d = 1 MM
△ d = 1.5 MM
○ d = 2 MM
REGION I
REGION II
E_p = 8 KeV
E_p = 7 KeV
E_p = 6 KeV
YIELD WITHOUT MULTIPLICATION
a
b
$\frac{a}{a+b}$ = FRACTION OF ELECTRONS MULTIPLYING
δ_t
V_S, VOLTS
889A3

Fig. 3

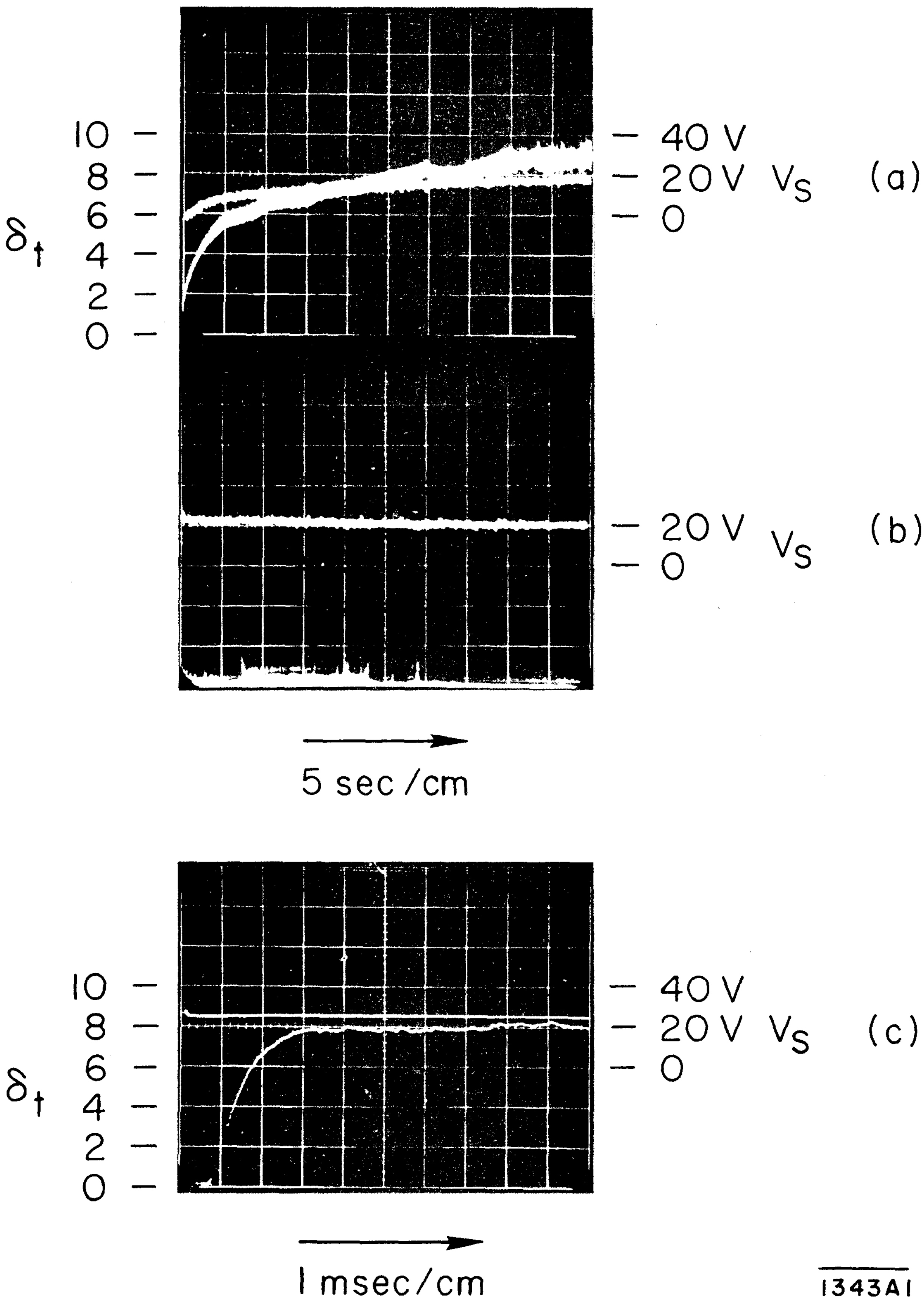
10
8
6
4
2
0
δt
40 V
20 V
0
Vs
(a)
20 V
0
Vs
(b)
5 sec/cm
10
8
6
4
2
0
δt
40 V
20 V
0
Vs
(c)
1 msec/cm
1343A1

Fig. 4

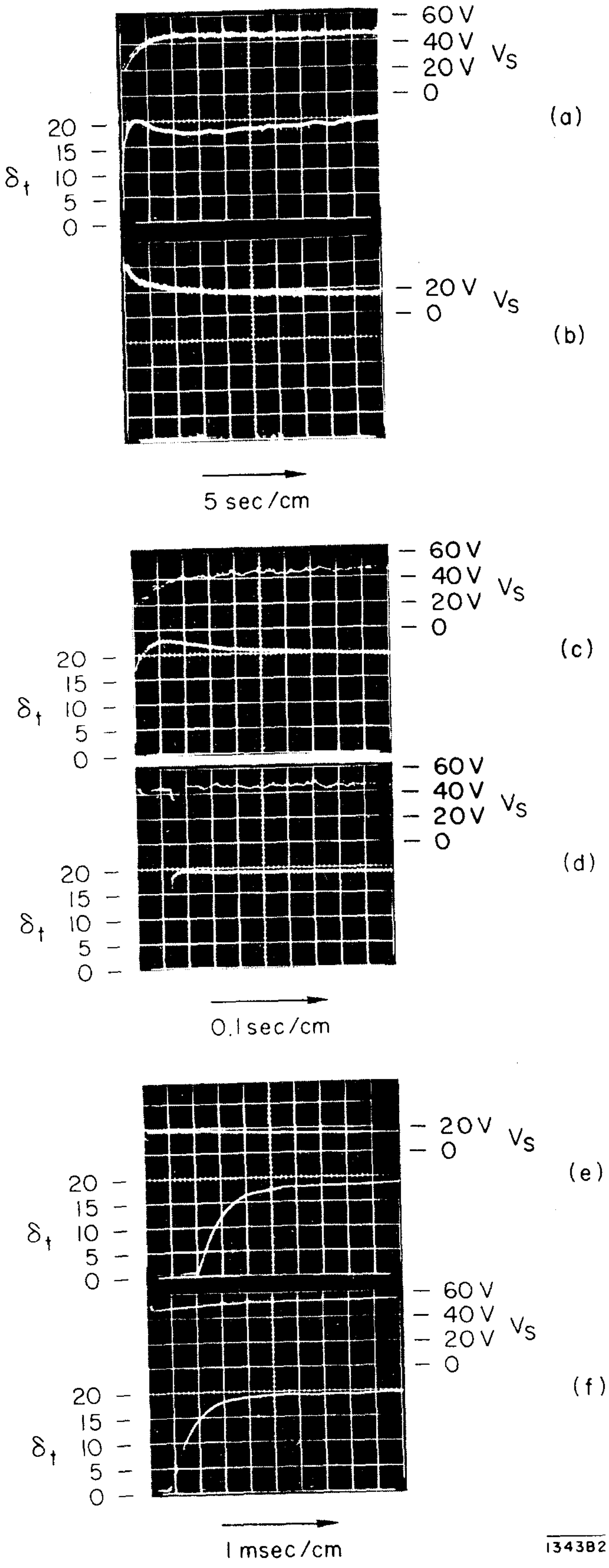

60 V
40 V
20 V
0
Vs
(a)
20
15
10
5
0
δt
20 V
0
Vs
(b)
5 sec/cm
60 V
40 V
20 V
0
Vs
(c)
20
15
10
5
0
δt
60 V
40 V
20 V
0
Vs
(d)
20
15
10
5
0
δt
0.1 sec/cm
20 V
0
Vs
(e)
20
15
10
5
0
δt
60 V
40 V
20 V
0
Vs
(f)
20
15
10
5
0
δt
1 msec/cm
134382

Fig. 5

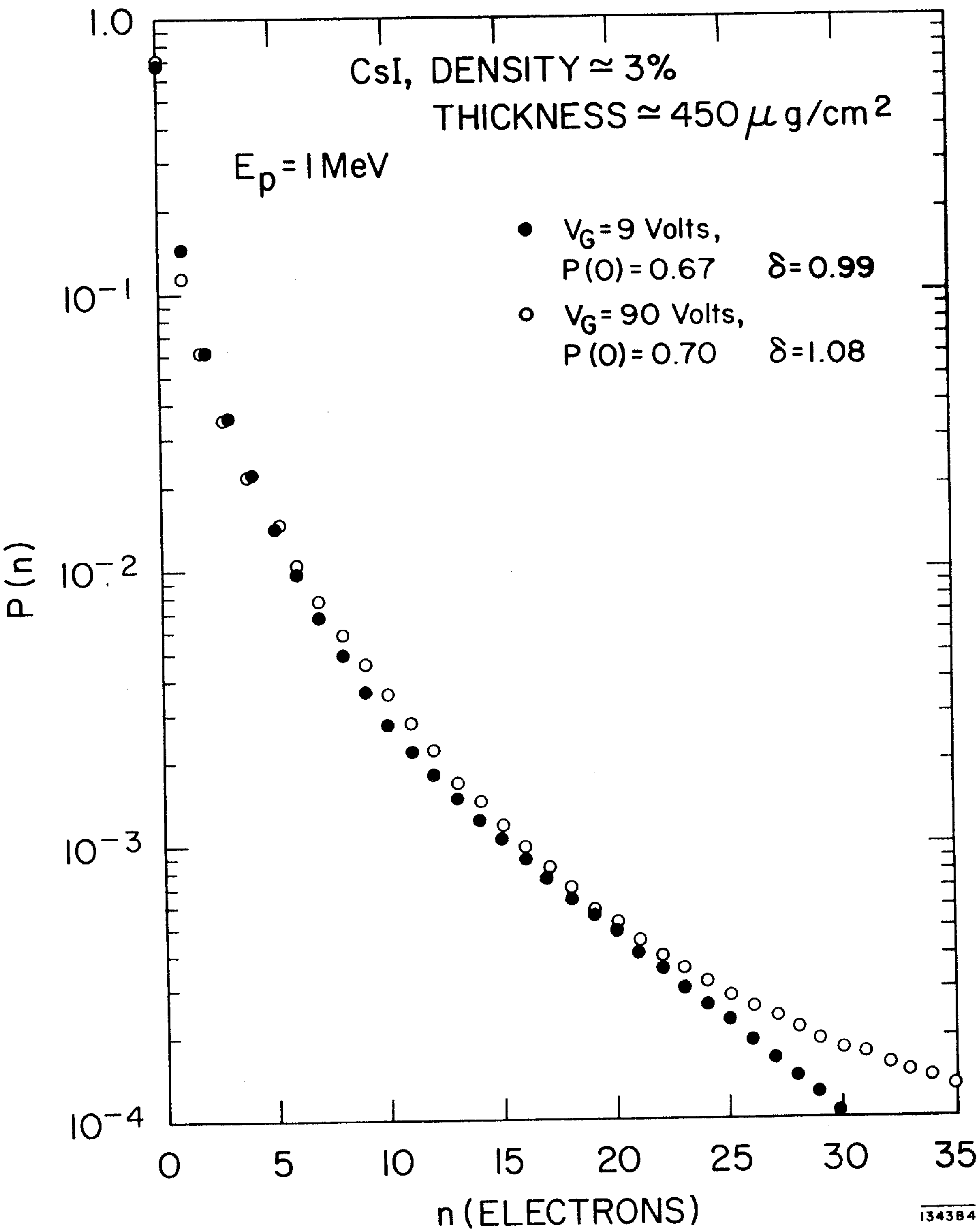

CsI, DENSITY ≃ 3%
THICKNESS ≃ 450 μg/cm²
E_p = 1 MeV
● V_G = 9 Volts, P(0) = 0.67 δ = 0.99
○ V_G = 90 Volts, P(0) = 0.70 δ = 1.08
1.0
10^{-1}
10^{-2}
10^{-3}
10^{-4}
P (n)
0
5
10
15
20
25
30
35
n (ELECTRONS)
134384

Fig. 6a

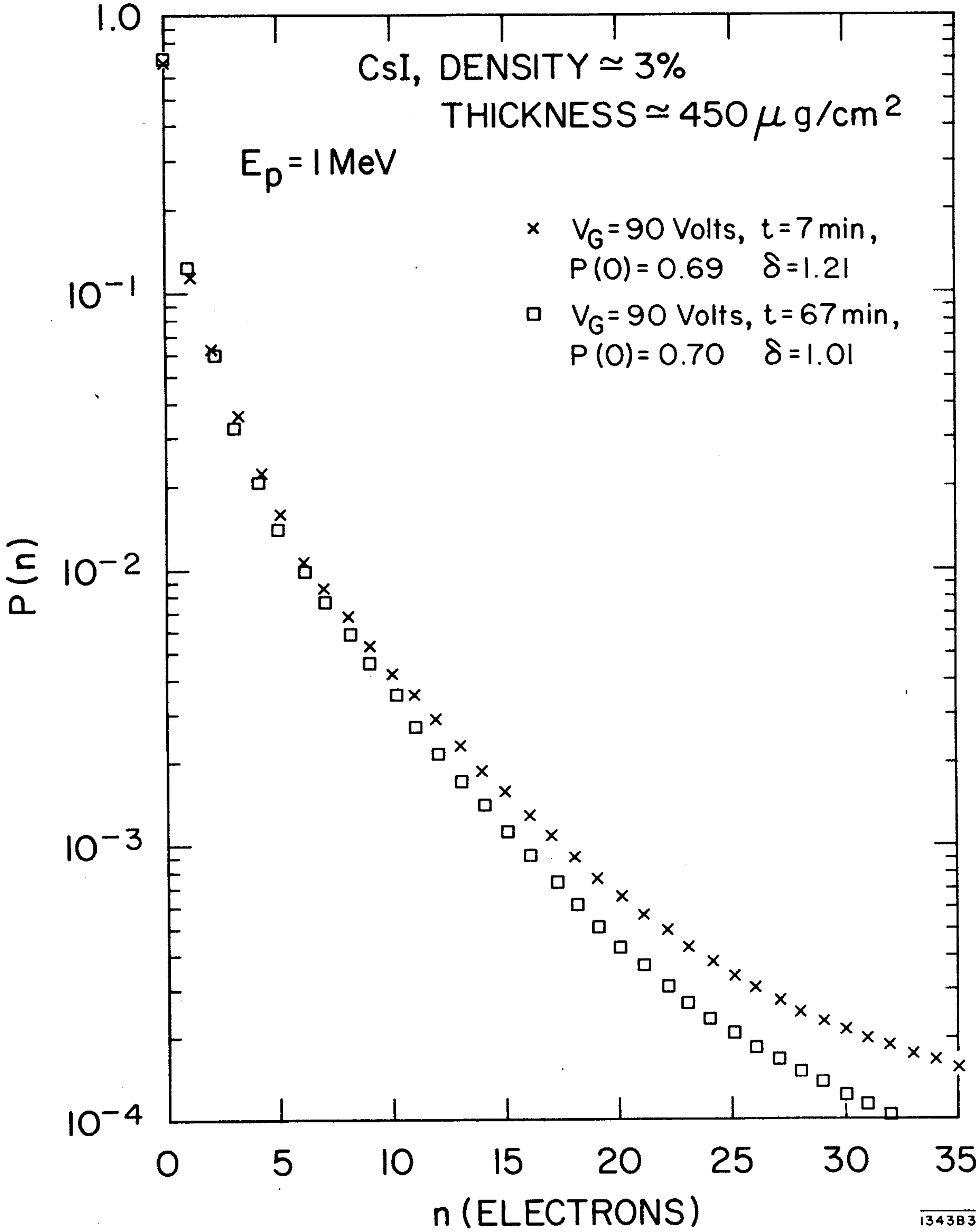
CsI, DENSITY ≃ 3%
THICKNESS ≃ 450 μg/cm²
E_p = 1 MeV
× V_G = 90 Volts, t = 7 min, P(0) = 0.69 δ = 1.21
□ V_G = 90 Volts, t = 67 min, P(0) = 0.70 δ = 1.01
P(n)
n (ELECTRONS)
1.0
10⁻¹
10⁻²
10⁻³
10⁻⁴
0
5
10
15
20
25
30
35
134383

Fig. 6b

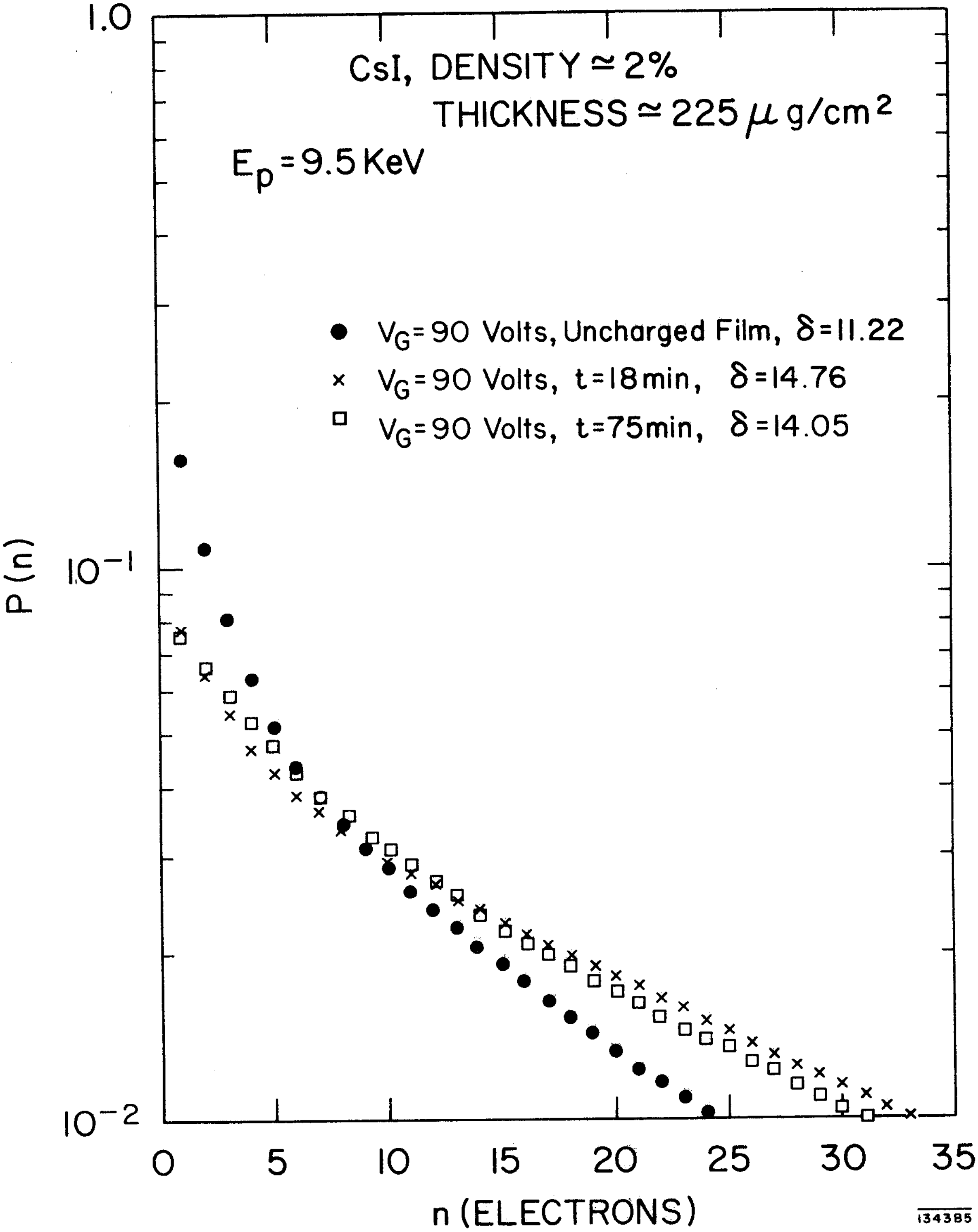

CsI, DENSITY ≃ 2%
THICKNESS ≃ 225 μg/cm²
E_p = 9.5 KeV
V_G = 90 Volts, Uncharged Film, δ = 11.22
V_G = 90 Volts, t = 18 min, δ = 14.76
V_G = 90 Volts, t = 75 min, δ = 14.05
P (n)
1.0
10⁻¹
10⁻²
0
5
10
15
20
25
30
35
n (ELECTRONS)
134385

Fig. 7

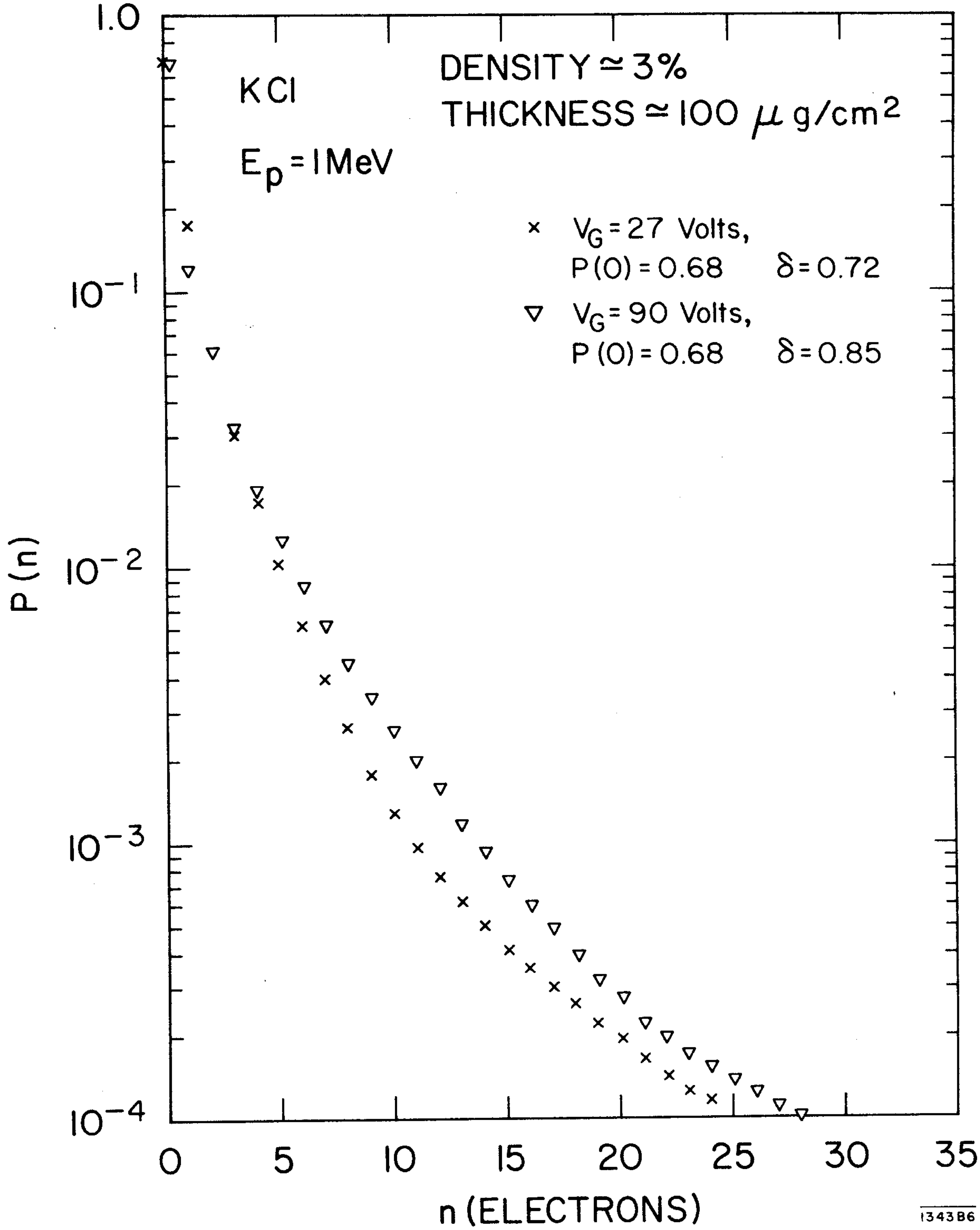

KCl
E_p = 1 MeV
DENSITY ≃ 3%
THICKNESS ≃ 100 μg/cm²
× V_G = 27 Volts, P(0) = 0.68 δ = 0.72
▽ V_G = 90 Volts, P(0) = 0.68 δ = 0.85
P(n)
1.0
10^{-1}
10^{-2}
10^{-3}
10^{-4}
0
5
10
15
20
25
30
35
n (ELECTRONS)
134386

Fig. 8

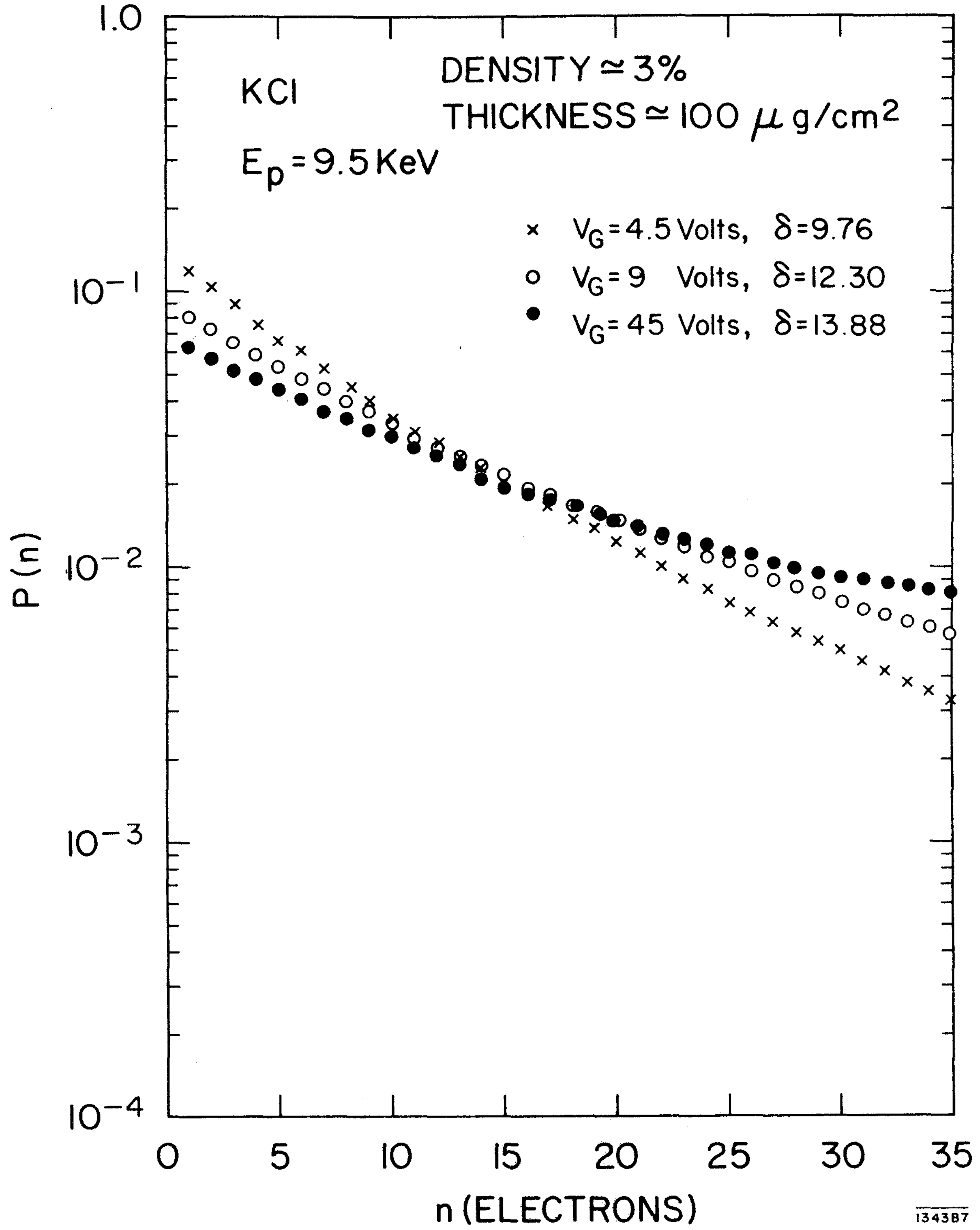

KCl
E_p = 9.5 KeV
DENSITY ≃ 3%
THICKNESS ≃ 100 μg/cm²
V_G = 4.5 Volts, δ = 9.76
V_G = 9 Volts, δ = 12.30
V_G = 45 Volts, δ = 13.88
1.0
10^{-1}
10^{-2}
10^{-3}
10^{-4}
P (n)
0
5
10
15
20
25
30
35
n (ELECTRONS)
134387

Fig. 9

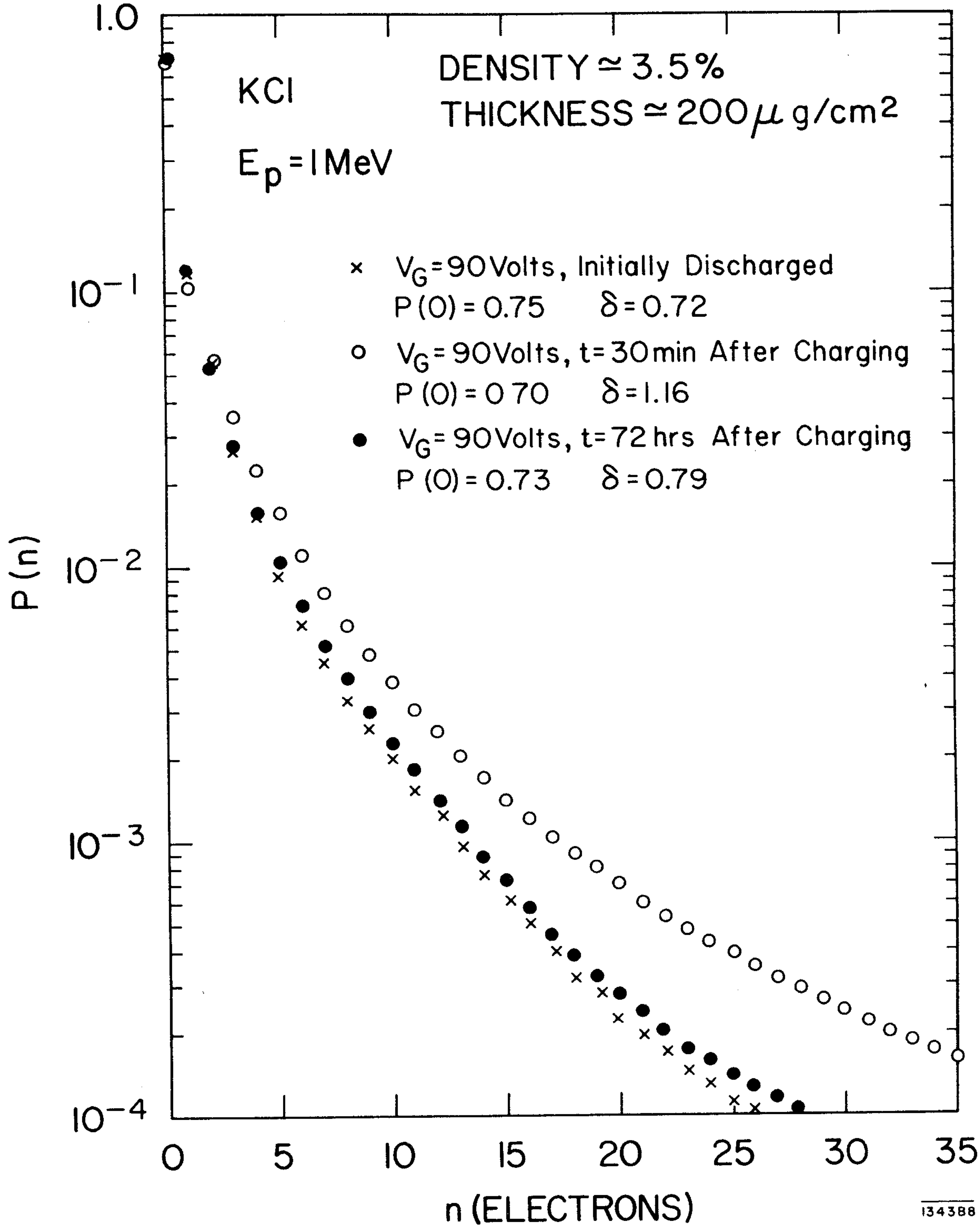

KCl
E_p = 1 MeV
DENSITY ≃ 3.5%
THICKNESS ≃ 200 μg/cm²
× V_G = 90 Volts, Initially Discharged
P (0) = 0.75 δ = 0.72
○ V_G = 90 Volts, t = 30 min After Charging
P (0) = 0 70 δ = 1.16
● V_G = 90 Volts, t = 72 hrs After Charging
P (0) = 0.73 δ = 0.79
P (n)
1.0
10⁻¹
10⁻²
10⁻³
10⁻⁴
0
5
10
15
20
25
30
35
n (ELECTRONS)
134388

Fig. 10

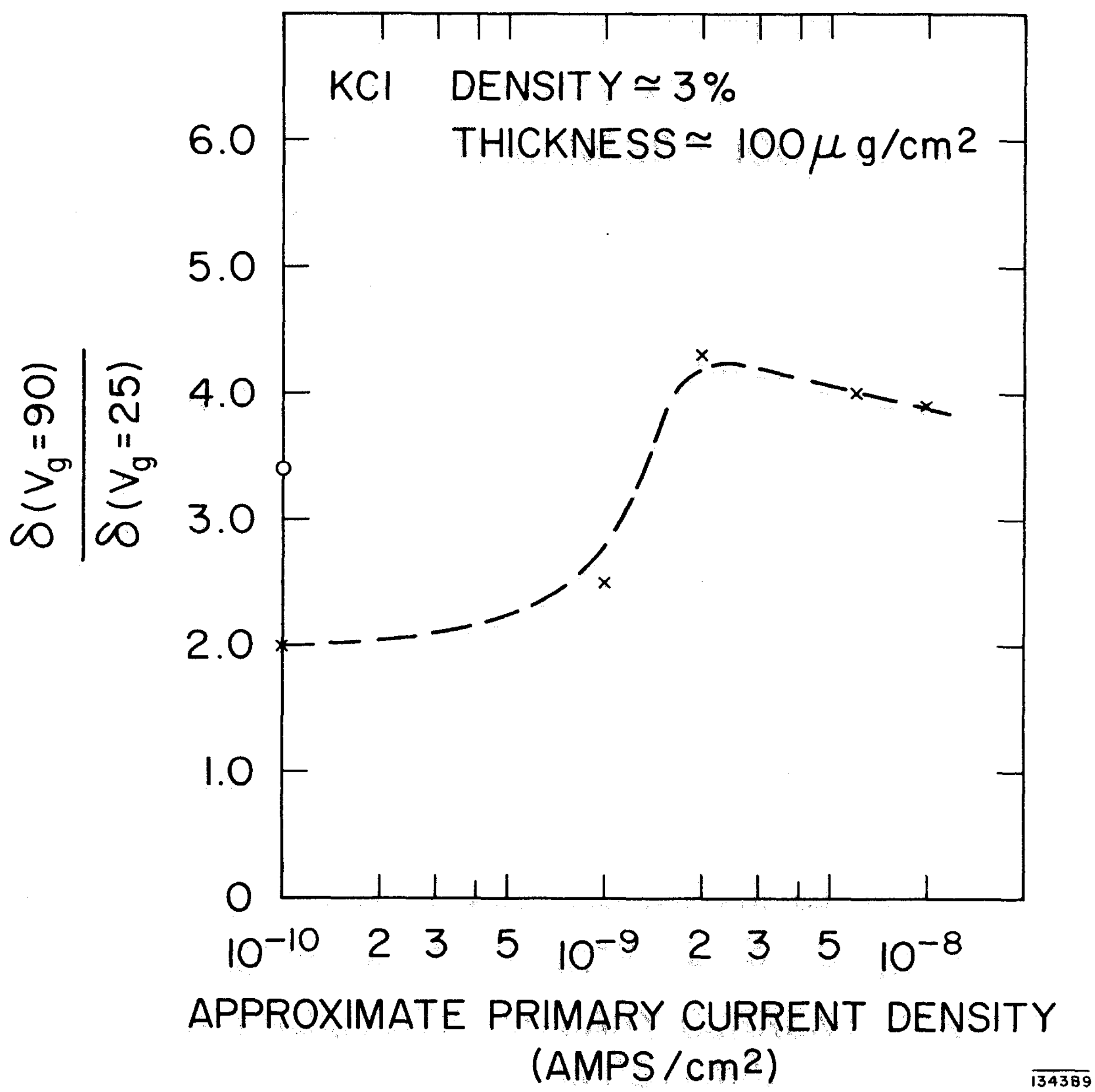
KCl DENSITY ≃ 3%
THICKNESS ≃ 100 μg/cm2
6.0
5.0
4.0
3.0
2.0
1.0
0
δ(Vg=90) / δ(Vg=25)
10−10 2 3 5 10−9 2 3 5 10−8
APPROXIMATE PRIMARY CURRENT DENSITY
(AMPS/cm2)
134389

Fig. 11

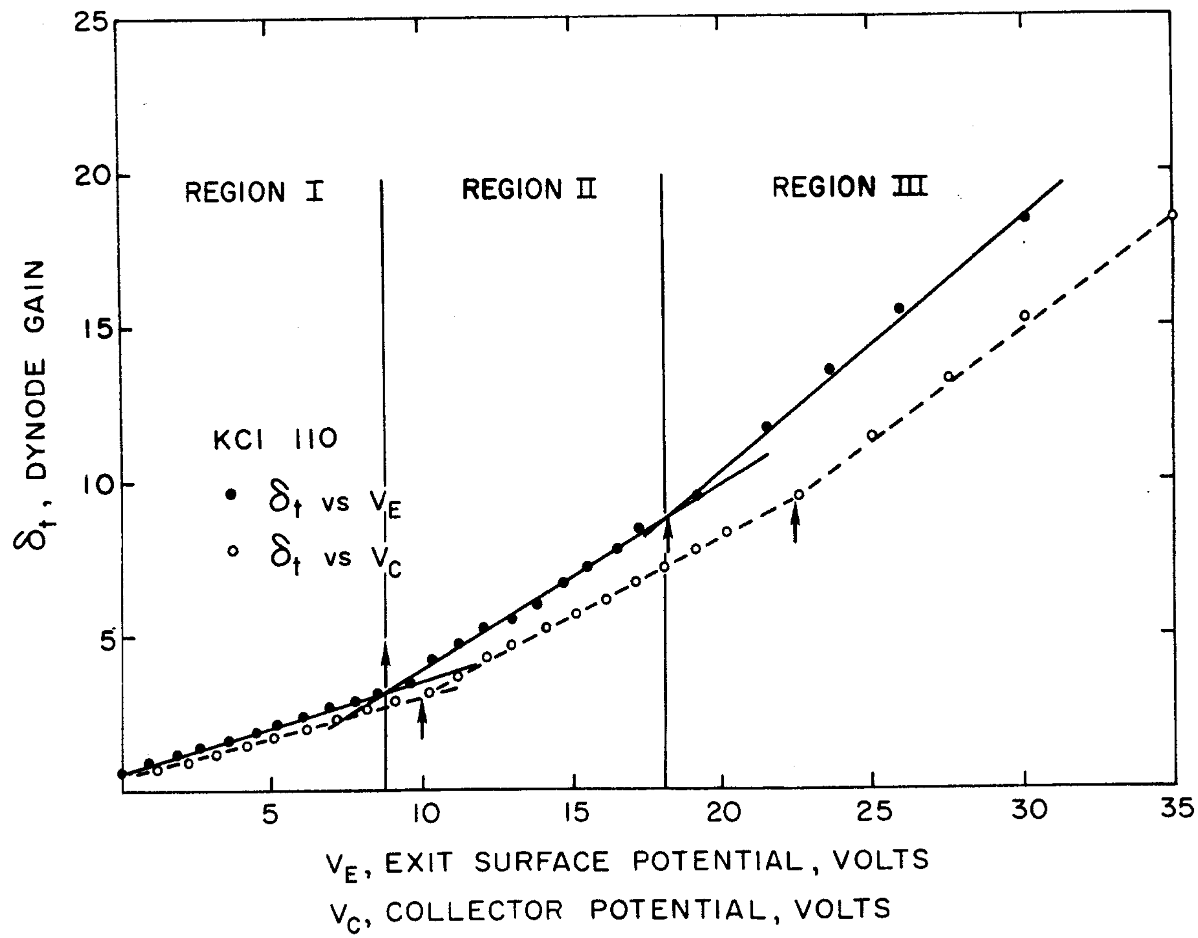
REGION I
REGION II
REGION III
KCl 110
δ_t vs V_E
δ_t vs V_C
δ_t, DYNODE GAIN
V_E, EXIT SURFACE POTENTIAL, VOLTS
V_C, COLLECTOR POTENTIAL, VOLTS
1343A10

Fig. 12